

Multispectral demosaicking using guided filter

Yusuke Monno^a, Masayuki Tanaka^a, Masatoshi Okutomi^a

^aTokyo Institute of Technology, 2-12-1 O-okayama, Meguro-ku, Tokyo, JAPAN;

ABSTRACT

Multispectral imaging is highly demanded for precise color reproduction and for various computer vision applications. Multispectral imaging with a multispectral color filter array (MCFA), which can be considered as a multispectral extension of commonly used consumer RGB cameras, could be a simple, low-cost, and practical system. A challenge of the multispectral imaging with the MCFA is multispectral demosaicking because each spectral component of the MCFA is severely undersampled. In this paper, we propose a novel multispectral demosaicking algorithm using a guided filter. The guided filter is recently proposed as an excellent structure-preserving filter. The guided filter requires so-called a guide image. A main issue of the guided filter is how to obtain an effective guide image. In our proposed algorithm, we generate the guide image from the most densely sampled spectral component in the MCFA. Then, other spectral components are interpolated by the guided filter. Experimental results demonstrate that our proposed algorithm outperforms other existing demosaicking algorithms both visually and quantitatively.

Keywords: Multispectral imaging, color filter array (CFA), demosaicking, guided filter

1. INTRODUCTION

Multispectral imaging is highly demanded for precise color reproduction and for various computer vision applications in many fields like medicine, agriculture, and remote sensing. By measuring more than three spectral components, multispectral imaging can provide better fidelity for image displays and remarkable advantages to many computer vision applications such as scene segmentation, object recognition, and relighting. However, existing systems for multispectral imaging are still impractical compared to commonly used consumer RGB cameras.

A wide variety of systems have been proposed for multispectral imaging. These systems can be broadly classified into three categories: (i) multi-camera-one-shot systems, (ii) single-camera-multi-shot systems, and (iii) single-camera-one-shot systems. Multi-camera-one-shot systems use multiple cameras with different color filters. Ohsawa *et al.* proposed a six-band HDTV camera which consists of a beam splitter and two RGB cameras with different color filters.¹ Although this camera can capture multispectral images at video frame rate, this camera should be expensive because perfectly aligned multiple cameras are required. Single-camera-multi-shot systems can be implemented by sequentially replacing color filters in front of a camera² or changing light sources.³⁻⁵ These systems can capture multispectral images at a high spectral resolution by replacing color filters or changing light sources many times. However, these systems require multiple shots to obtain multispectral images. To capture multispectral images at video frame rate, high-speed lighting equipment such as specially designed LED clusters or a DLP projector is required.^{4,5}

Single-camera-one-shot systems use a single image sensor with a multispectral color filter array (MCFA), in which more than three spectral components are arrayed.⁶⁻⁹ These systems can be considered as a multispectral extension of commonly used consumer RGB cameras. In these systems, full-multispectral images are needed to be interpolated from the raw data observed by the single image sensor with a CFA.^{10,11} This interpolation process is called demosaicking. In this paper, the demosaicking process for the MCFA is referred to as multispectral demosaicking. Compared to the previous two categories, single-camera-one-shot systems provide significant

Further author information: (Send correspondence to Y.Monno)

Y.Monno: E-mail: ymonno@ok.ctrl.titech.ac.jp, Telephone: +81-3-5734-3499

M.Tanaka: E-mail: mtanaka@ctrl.titech.ac.jp, Telephone: +81-3-5734-3270

M.Okutomi: E-mail: mxo@ctrl.titech.ac.jp, Telephone: +81-3-5734-3472

advantages of low-cost and simple video acquisition. However, multispectral demosaicking has been a challenging problem because each spectral component is severely undersampled.

Various demosaicking algorithms have been proposed.^{10,11} However, almost all these algorithms are intended for a single RGB camera with the Bayer CFA.¹² Although demosaicking algorithms for an arbitrary CFA have been proposed,^{13–15} these algorithms are mainly discussed for RGB demosaicking. To our knowledge, few algorithms address the multispectral demosaicking problem.^{6–9} Baone and Qi proposed a MAP-based multispectral demosaicking algorithm.⁶ Brauers and Aach obtained full-multispectral images by lowpass filtering of color differences.⁷ Miao *et al.* performed edge-sensing interpolation to each spectral component.⁸ In our previous work, we proposed adaptive kernel upsampling to effectively interpolate each spectral component from a direction along an edge.⁹ Nevertheless, multispectral demosaicking results by these existing algorithms still have visible artifacts especially in edges.

In this paper, we propose a novel multispectral demosaicking algorithm. We use a guided filter to interpolate each spectral component. The guided filter is recently proposed as an excellent structure-preserving filter.¹⁶ The guided filter requires so-called a guide image. The output of the guided filter can be represented as a linear transform of the guide image, thus it nicely resembles the guide image. Therefore, a main issue of the guided filter is how to obtain an effective guide image. In our proposed algorithm, the guide image is generated from the most densely sampled spectral component in the MCFA. Then, other spectral components are interpolated by the guided filter. We experimentally demonstrate that our proposed algorithm outperforms other existing demosaicking algorithms both visually and quantitatively.

2. GUIDED FILTER

The guided filter is recently proposed as an excellent structure-preserving filter.¹⁶ The guided filter generates the output by a linear transform of a given guide image. In the guided filter, the filter output in each window is modeled by the linear transformation of the guide image as:

$$q_{\mathbf{x}_i} = a_{\mathbf{x}_p} I_{\mathbf{x}_i} + b_{\mathbf{x}_p}, \quad \forall \mathbf{x}_i \in \omega_{\mathbf{x}_p}, \quad (1)$$

where $\omega_{\mathbf{x}_p}$ denotes the window centered at the pixel location \mathbf{x}_p , \mathbf{x}_i is a pixel location in the window, $q_{\mathbf{x}_i}$ is the filter output at the location \mathbf{x}_i , and $I_{\mathbf{x}_i}$ is the intensity of the guide image at the location \mathbf{x}_i . Linear coefficients $(a_{\mathbf{x}_p}, b_{\mathbf{x}_p})$ for each window are estimated by minimizing the cost function:

$$E(a_{\mathbf{x}_p}, b_{\mathbf{x}_p}) = \sum_{\mathbf{x}_i \in \omega_{\mathbf{x}_p}} M_{\mathbf{x}_i} ((a_{\mathbf{x}_p} I_{\mathbf{x}_i} + b_{\mathbf{x}_p} - p_{\mathbf{x}_i})^2 + \epsilon a_{\mathbf{x}_p}^2), \quad (2)$$

where $p_{\mathbf{x}_i}$ is the intensity of the input image at the location \mathbf{x}_i , $M_{\mathbf{x}_i}$ is a binary mask at the location \mathbf{x}_i , and ϵ is a smoothing parameter. The binary mask is set to one if data is sampled at an associated location and set to zero for other cases. The location \mathbf{x}_i is involved in the windows that contain the location \mathbf{x}_i , thus the final output at the location \mathbf{x}_i is calculated by averaging as:

$$q_{\mathbf{x}_i} = \bar{a}_{\mathbf{x}_i} I_{\mathbf{x}_i} + \bar{b}_{\mathbf{x}_i}, \quad (3)$$

where $\bar{a}_{\mathbf{x}_i} = \frac{1}{|\omega|} \sum_{\mathbf{x}_p \in \omega_{\mathbf{x}_i}} a_{\mathbf{x}_p}$, $\bar{b}_{\mathbf{x}_i} = \frac{1}{|\omega|} \sum_{\mathbf{x}_p \in \omega_{\mathbf{x}_i}} b_{\mathbf{x}_p}$, and $|\omega|$ is the number of pixels in the window.

3. PROPOSED ALGORITHM

In this section, we describe the details of our proposed multispectral demosaicking algorithm. We use the guided filter to interpolate each spectral component to obtain full-multispectral images. The key to effective interpolation by the guided filter is to obtain an effective guide image. In our proposed algorithm, we take advantages of the MCFA which we have proposed⁹ to generate the effective guide image.

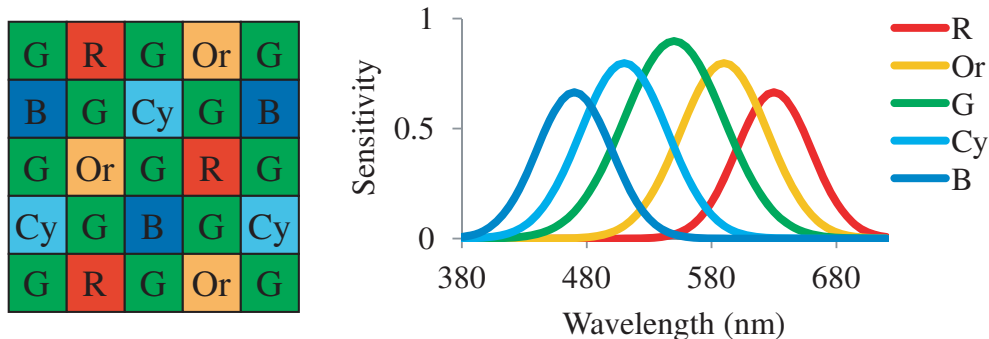


Figure 1. Our proposed MCFA and the corresponding schematic spectral sensitivities of each spectral band.

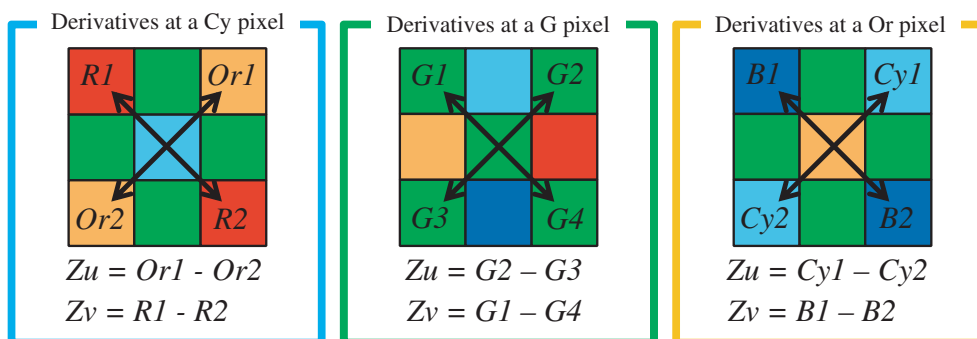


Figure 2. The examples of diagonal derivatives at a Or, G, and Cy-pixel location.

3.1 Multispectral color filter array and direct adaptive kernel estimation

In our multispectral demosaicking, we use the MCFA which we have proposed in the literature.⁹ Fig. 1 shows our proposed MCFA and the corresponding schematic spectral sensitivities of each spectral band. In this paper, we call each spectral band R, Or, G, Cy, and B-band respectively from the long-wavelength side to the short-wavelength side. There are two advantages in our proposed MCFA: (i) the sampling density of the G-band data is as high as the Bayer CFA, (ii) an adaptive kernel can be estimated directly from the raw data observed by our proposed MCFA. These two advantages are used to obtain the effective guide image.

The first advantage of our proposed MCFA is that the sampling density of the G-band data is as high as the Bayer CFA. In the guided filter, the output resembles the guide image. Therefore, the guide image is needed to be generated effectively. To this end, we generate the guide image from the G-band data because high-performance interpolation is expected for the G-band data.

The second advantage of the proposed MCFA is that the adaptive kernel can be estimated directly from the raw data observed by our proposed MCFA. The adaptive kernel is proposed by Takeda *et al.* for kernel regression.¹⁷ The adaptive kernel is also used for high-performance upsampling.⁹ We apply the adaptive Gaussian upsampling⁹ to interpolate the G-band data to generate the effective guide image.

In our proposed MCFA, the adaptive kernel is estimated based on the assumption that derivatives of each spectral band are approximately equivalent. Based on this assumption, derivatives can be calculated in diagonal directions at all pixel locations. Fig. 2 shows the examples of diagonal derivatives at a Or, G, and Cy-pixel location. Using these diagonal derivatives, the adaptive kernel at the location \mathbf{x}_p can be estimated directly from the raw data as:

$$k_{\mathbf{x}_p}(\mathbf{x}) = \exp \left[-\frac{\mathbf{x}^T \mathbf{H}^T \mathbf{C}_{\mathbf{x}_p}^{-1} \mathbf{H} \mathbf{x}}{2h^2} \right], \quad (4)$$

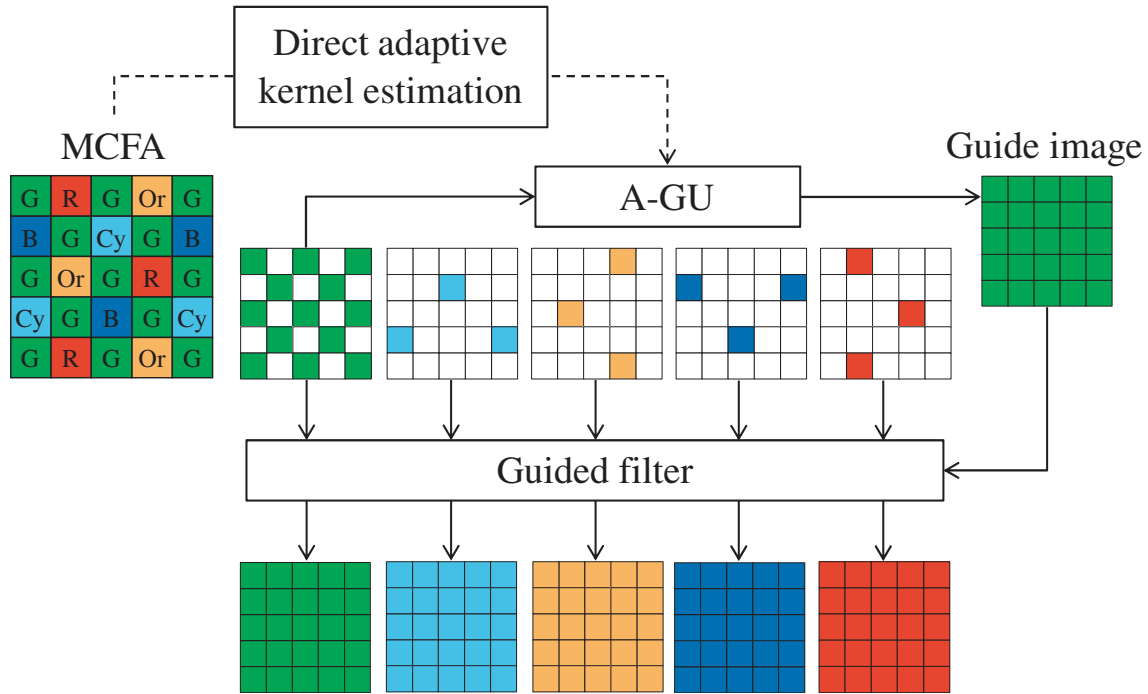


Figure 3. The schematic block diagram of our proposed algorithm.

where $\mathbf{C}_{\mathbf{x}_p}$ is the covariance matrix of the Gaussian kernel, h stands for a smoothing parameter, which controls the kernel size, and \mathbf{H} is the matrix which aligns the pixel coordinates with the direction of the derivatives. Specifically, we use the rotation matrix which rotates the pixel coordinates by 45 degrees. The covariance matrix $\mathbf{C}_{\mathbf{x}_p}$ is estimated based on the diagonal derivatives around the location \mathbf{x}_p as:

$$\mathbf{C}_{\mathbf{x}_p}^{-1} = \frac{1}{|\mathbf{N}_{\mathbf{x}_p}|} \begin{pmatrix} \sum_{\mathbf{x}_j \in \mathbf{N}_{\mathbf{x}_p}} z_u(\mathbf{x}_j) z_u(\mathbf{x}_j) & \sum_{\mathbf{x}_j \in \mathbf{N}_{\mathbf{x}_p}} z_u(\mathbf{x}_j) z_v(\mathbf{x}_j) \\ \sum_{\mathbf{x}_j \in \mathbf{N}_{\mathbf{x}_p}} z_u(\mathbf{x}_j) z_v(\mathbf{x}_j) & \sum_{\mathbf{x}_j \in \mathbf{N}_{\mathbf{x}_p}} z_v(\mathbf{x}_j) z_v(\mathbf{x}_j) \end{pmatrix}, \quad (5)$$

where z_u and z_v are the diagonal derivatives, $\mathbf{N}_{\mathbf{x}_p}$ denotes neighbor pixels around the location \mathbf{x}_p , and $|\mathbf{N}_{\mathbf{x}_p}|$ is the pixel number of $\mathbf{N}_{\mathbf{x}_p}$. In this paper, this estimation process of the adaptive kernel from the raw data is referred to as a direct adaptive kernel estimation.

3.2 Multispectral demosaicking using guided filter

The schematic block diagram of our proposed algorithm is shown in Fig. 3. First, the guide image to be used for the guided filter is generated from the G-band data, which is the most densely sampled component in our proposed MCFA. Then, the guided filter is applied to interpolate each spectral component. We apply the adaptive Gaussian upsampling (A-GU in Fig. 3)⁹ to interpolate the G-band data to generate the guide image. The adaptive Gaussian upsampling is applied based on the adaptive kernel, which is estimated by the direct adaptive kernel estimation as described in previous section. The upsampled result of the adaptive Gaussian upsampling $S_{\mathbf{x}_p}^{GU}$ at the location \mathbf{x}_p is obtained as:

$$S_{\mathbf{x}_p}^{GU} = \frac{1}{w_{\mathbf{x}_p}} \sum_{\mathbf{x}_i \in \mathbf{N}_{\mathbf{x}_p}} k_{\mathbf{x}_p}(\mathbf{x}_i - \mathbf{x}_p) M_{\mathbf{x}_i} S_{\mathbf{x}_i}, \quad (6)$$

where $S_{\mathbf{x}_i}$ is the sampled value at the location \mathbf{x}_i , $M_{\mathbf{x}_i}$ is the binary mask at the location \mathbf{x}_i , and $w_{\mathbf{x}_p}$ is the normalizing factor, which is sum of kernel weights.

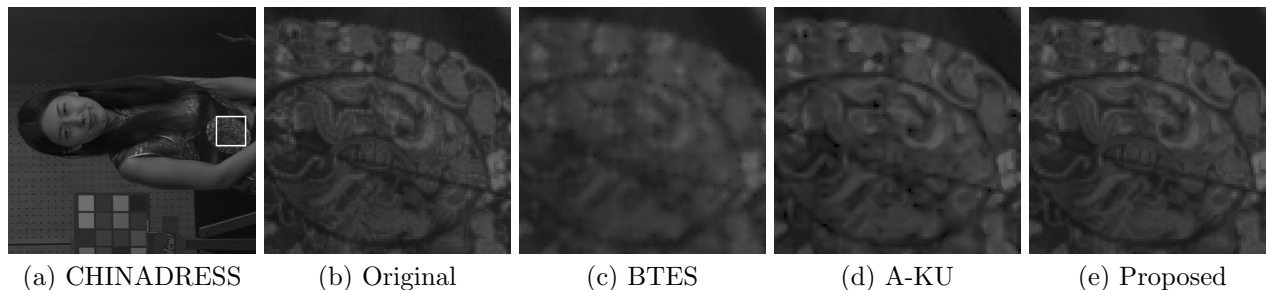


Figure 4. Visual comparison of B-band images on a part of CHINADDRESS. (Gamma correction is applied for the display.)

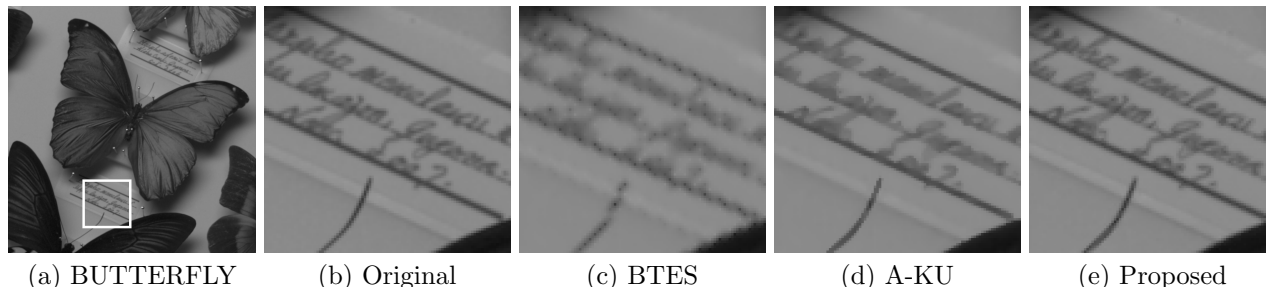


Figure 5. Visual comparison of Or-band images on a part of BUTTERFLY. (Gamma correction is applied for the display.)

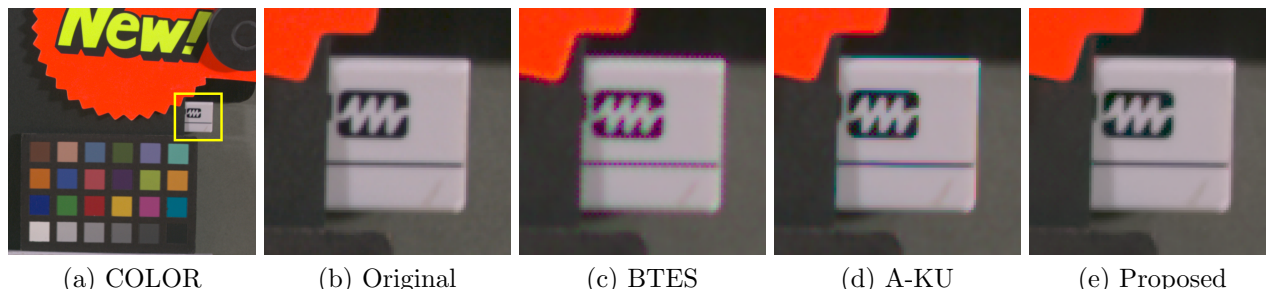


Figure 6. Visual comparison of sRGB images on a part of COLOR. (Gamma correction is applied for the display.)

4. EXPERIMENTS

We compare our proposed algorithm with existing multispectral demosaicking algorithms and existing Bayer demosaicking algorithms. For experimental comparisons, five-band multispectral images are captured and used as original five-band images. Then, original standard RGB (sRGB) images are converted from the original five-band images for visual comparisons in color images. We use the spatio-spectral Wiener estimation¹⁸ to estimate the matrix which converts five-band images to sRGB images. We experimentally validate with 16 scenes.

First, we compare our proposed algorithm with existing multispectral demosaicking algorithms. Original five-band images are sampled assuming the proposed MCFA and demosaicked by three multispectral demosaicking algorithms: (i) the binary tree-based edge-sensing (BTES) algorithm,⁸ (ii) the adaptive kernel upsampling (A-KU) algorithm,⁹ and (iii) our proposed algorithm. Then, sRGB images are converted from the demosaicked five-band images. In our proposed algorithm, the smoothing parameter h is set to 1, ϵ is set to 0, the kernel size for the adaptive Gaussian upsampling is set to 3×3 , and the window size for the guided filter is set to 9×9 .

Fig. 4 shows the demosaicked Or-band images of CHINADDRESS and Fig. 5 shows the demosaicked B-band images of BUTTERFLY. These results demonstrate that our proposed algorithm can effectively reproduce edges and textures compared to the other existing algorithms. Fig. 6 shows the sRGB images converted from the demosaicked five-band images of COLOR. These sRGB images show that our proposed algorithm effectively reduces color artifacts in edges.

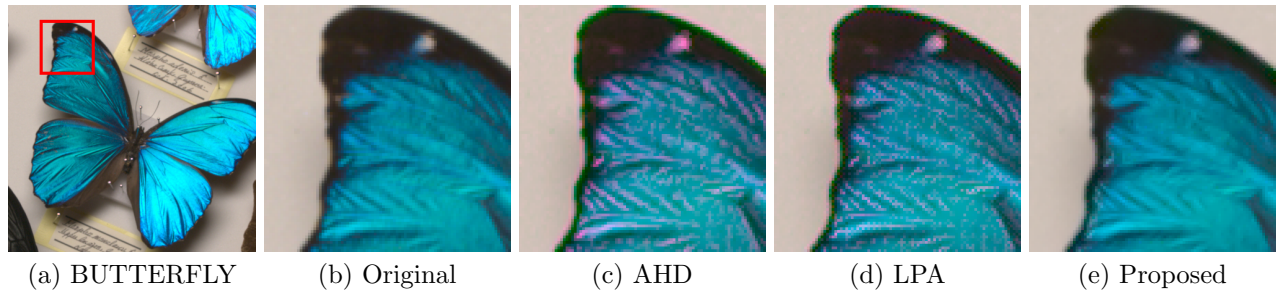


Figure 7. Visual comparison of sRGB images on a part of BUTTERFLY. (Gamma correction is applied for the display.)

Table 1. PSNR(dB) performances of the different demosaicking algorithms for CHINADDRESS, BUTTERFLY, COLOR, and the average PSNR of 16 scenes, where the bold typeface represents the highest PSNR.

| Image index | Demosaicking algorithm | Band index | | | | | | | |
|----------------------|------------------------|--------------|--------------|--------------|--------------|--------------|--------------|--------------|--------------|
| | | R | Or | G | Cy | B | sR | sG | sB |
| CHINADDRESS | AHD | - | - | - | - | - | 31.45 | 39.24 | 35.71 |
| | LPA | - | - | - | - | - | 33.39 | 42.32 | 38.30 |
| | BTES | 48.53 | 44.09 | 49.24 | 47.34 | 49.38 | 33.28 | 44.06 | 40.73 |
| | A-KU | 52.74 | 47.17 | 49.31 | 50.05 | 52.47 | 37.07 | 45.09 | 43.71 |
| | Proposed | 52.74 | 50.33 | 50.28 | 53.11 | 54.02 | 39.75 | 46.56 | 45.52 |
| BUTTERFLY | AHD | - | - | - | - | - | 27.22 | 36.15 | 34.20 |
| | LPA | - | - | - | - | - | 29.33 | 39.04 | 36.08 |
| | BTES | 45.71 | 42.20 | 45.29 | 37.57 | 40.54 | 31.11 | 40.29 | 32.44 |
| | A-KU | 50.48 | 46.24 | 46.70 | 41.88 | 45.17 | 36.11 | 42.29 | 37.34 |
| | Proposed | 52.48 | 50.30 | 47.33 | 45.02 | 45.86 | 40.11 | 44.15 | 38.33 |
| COLOR | AHD | - | - | - | - | - | 29.71 | 39.85 | 36.86 |
| | LPA | - | - | - | - | - | 30.98 | 41.83 | 38.92 |
| | BTES | 47.34 | 43.60 | 50.17 | 44.23 | 46.50 | 32.53 | 43.49 | 37.94 |
| | A-KU | 51.23 | 46.97 | 53.32 | 47.31 | 50.06 | 35.87 | 45.83 | 41.68 |
| | Proposed | 50.54 | 49.02 | 54.17 | 51.29 | 52.07 | 37.83 | 47.97 | 43.61 |
| Average of 16 scenes | AHD | - | - | - | - | - | 28.80 | 38.59 | 34.47 |
| | LPA | - | - | - | - | - | 30.39 | 41.24 | 36.71 |
| | BTES | 49.38 | 45.00 | 48.60 | 42.78 | 44.93 | 34.46 | 42.95 | 36.36 |
| | A-KU | 52.19 | 47.80 | 48.78 | 45.38 | 48.06 | 38.14 | 44.20 | 39.53 |
| | Proposed | 53.12 | 51.06 | 49.61 | 47.94 | 48.89 | 40.75 | 45.73 | 40.51 |

Next, we compare our proposed algorithm with existing Bayer demosaicking algorithms. For Bayer demosaicking, Bayer CFA mosaic images are simulated using only the original R, G, and B-band images. Then, the Bayer CFA mosaic images are demosaicked by two algorithms: (i) the local polynomial approximation (LPA) algorithm,¹⁹ (ii) the adaptive homogeneity-directed (AHD) algorithm.²⁰ These two algorithms are known as high-performance demosaicking algorithms for the Bayer CFA. For visual comparisons with the sRGB images converted from the demosaicked five-band images by our proposed algorithm, the demosaicked RGB images are also converted to sRGB images.

Fig. 7 shows the sRGB images converted from the demosaicked five-band images and the demosaicked RGB images. These sRGB images demonstrate that our proposed algorithm correctly reproduces color, while the converted images from the demosaicked RGB images have color artifacts on the butterfly wing. Please see more results at <http://www.ok.ctrl.titech.ac.jp/res/MSI/GF.html>.

Finally, we evaluate PSNR performances of the demosaicked images by the different demosaicking algorithms. Table 1 shows the PSNR(dB) performances for BUTTERFLY, CHINADDRESS, COLOR, and the average PSNR of 16 scenes. Our proposed algorithm outperforms the other algorithms in both five-bands and sRGB-bands. These PSNR performances show the effectiveness of our proposed algorithm quantitatively.

5. CONCLUSION

In this paper, we have proposed a novel multispectral demosaicking algorithm. We use the guided filter to interpolate each spectral component. In the guided filter, the key to effective interpolation is to obtain the effective guide image. In our proposed algorithm, we take advantages of our proposed MCFA to generate the effective guide image. First, we generate the guide image from the most densely sampled spectral component in the MCFA. Then, other spectral components are interpolated by the guided filter. The experimental results demonstrate that our proposed algorithm effectively reproduces edges and textures and reduces color artifacts.

REFERENCES

- [1] Ohsawa, K., Ajito, T., Fukuda, H., Komiya, Y., Haneishi, H., Yamaguchi, M., and Ohya, N., "Six-band HDTV camera system for spectrum-based color reproduction," *Journal of Imaging Science and Technology* **48**(2), 85–92 (2004).
- [2] Fukuda, H., Uchiyama, T., Haneishi, H., Yamaguchi, M., and Ohya, N., "Development of 16-bands multispectral image archiving system," *Proc. of SPIE* **5667**, 136–145 (2005).
- [3] Cui, C., Yoo, H., and Ben-Ezra, M., "Multi-spectral imaging by optimized wide band illumination," *International Journal of Computer Vision* **86**(2-3), 140–151 (2010).
- [4] Park, J., Lee, M., Grossberg, M. D., and Nayar, S. K., "Multispectral imaging using multiplexed illumination," *Proc. of IEEE International Conference on Computer Vision (ICCV)*, 1–8 (2007).
- [5] Han, S., Sato, I., Okabe, T., and Sato, Y., "Fast spectral reflectance recovery using DLP projector," *Proc. of Asian Conference on Computer Vision (ACCV)* **1**, 318–330 (2010).
- [6] Baone, G. and Qi, H., "Demosaicking methods for multispectral cameras using mosaic focal plane array technology," *Proc. of SPIE* **6062**, 75–87 (2006).
- [7] Brauers, J. and Aach, T., "A color filter array based multispectral camera," *12. Workshop Farbbildverarbeitung* (2006).
- [8] Miao, L., Qi, H., Ramanath, R., and Snyder, W. E., "Binary tree-based generic demosaicking algorithm for multispectral filter arrays," *IEEE Transactions on Image Processing* **15**, 3550–3558 (2006).
- [9] Monno, Y., Tanaka, M., and Okutomi, M., "Multispectral demosaicking using adaptive kernel upsampling," *Proc. of IEEE International Conference on Image Processing (ICIP)*, 3218–3221 (2011).
- [10] Li, X., Gunturk, B., and Zhang, L., "Image demosaicking: a systematic survey," *Proc. of SPIE* **6822**, 68221J–68221J–15 (2008).
- [11] Gunturk, B. K., Glotzbach, J., Altunbasak, Y., Schafer, R. W., and Mersereau, R. M., "Demosaicking: color filter array interpolation," *IEEE Signal Processing Magazine* **22**, 44–54 (2005).
- [12] Bayer, B., "Color imaging array," *US Patent 3971065* (1976).
- [13] Lukac, R. and Plataniotis, K. N., "Universal demosaicking for imaging pipelines with an rgb color filter array," *Pattern Recognition* **38**(11), 2208–2212 (2005).
- [14] Condat, L., "A generic variational approach for demosaicking from an arbitrary color filter array," *Proc. of IEEE International Conference on Image Processing (ICIP)*, 1625–1628 (2009).
- [15] Gu, J., Wolfe, P. J., and Hiraoka, K., "Filterbank-based universal demosaicking," *Proc. of IEEE International Conference on Image Processing (ICIP)*, 1981–1984 (2010).
- [16] He, K., Sun, J., and Tang, X., "Guided image filtering," *Proc. of the 11th European Conference on Computer Vision (ECCV)* **6311**, 1–14 (2010).
- [17] Takeda, H., Farsiu, S., and Milanfar, P., "Kernel regression for image processing and reconstruction," *IEEE Transactions on Image Processing* **16**, 349–366 (2007).
- [18] Murakami, Y., Fukura, K., Yamaguchi, M., and Ohya, N., "Color reproduction from low-SNR multispectral images using spatio-spectral wiener estimation," *Optics Express* **16**(6), 4106–4120 (2008).
- [19] Paliy, D., Katkovnik, V., Bilcu, R., Alenius, S., and Egiazarian, K., "Spatially adaptive color filter array interpolation for noiseless and noisy data," *International Journal of Imaging Systems and Technology* **17**, 105–122 (2007).
- [20] Hiraoka, K. and Parks, T. W., "Adaptive homogeneity-directed demosaicking algorithm," *IEEE Transactions on Image Processing* **14**, 360–369 (2005).